

## General Disclaimer

### One or more of the Following Statements may affect this Document

- This document has been reproduced from the best copy furnished by the organizational source. It is being released in the interest of making available as much information as possible.
- This document may contain data, which exceeds the sheet parameters. It was furnished in this condition by the organizational source and is the best copy available.
- This document may contain tone-on-tone or color graphs, charts and/or pictures, which have been reproduced in black and white.
- This document is paginated as submitted by the original source.
- Portions of this document are not fully legible due to the historical nature of some of the material. However, it is the best reproduction available from the original submission.

X-682-77-136

PREPRINT

*Tmx-71341*

**ON THREE-DIMENSIONAL  
RECONSTRUCTION OF OPTICALLY  
THIN SOLAR EMISSION SOURCES**

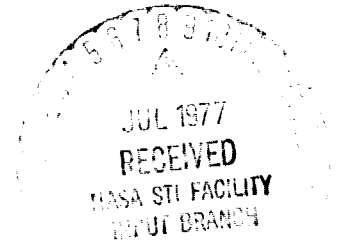
(NASA-TM-X-71341) ON THREE-DIMENSIONAL  
RECONSTRUCTION OF OPTICALLY THIN SOLAR  
EMISSION SOURCES (NASA) 23 p HC A02/MF A01  
CSCL 03B

N77-27056

Unclas  
G3/92 37032

**S. O. KASTNER  
R. J THOMAS  
C. WADE**

**MAY 1977**



**GODDARD SPACE FLIGHT CENTER  
GREENBELT, MARYLAND**

ON THREE-DIMENSIONAL RECONSTRUCTION  
OF OPTICALLY THIN SOLAR EMISSION SOURCES

S. O. Kastner, R. J. Thomas and C. Wade

Laboratory for Solar Physics and Astrophysics  
NASA-Goddard Space Flight Center  
Greenbelt, Maryland

May 1977

## ABSTRACT

An interim report is given of a calculation aimed at reconstructing the three-dimensional distribution of optically thin EUV emission sources associated with solar active regions, from two-dimensional observations (projections) recorded by the Goddard spectroheliograph on the OSO-7 satellite. Its relation to other image reconstruction methods in the literature is briefly discussed, together with special requirements imposed in the solar case such as a knowledge of the true solar rotation function. A useful correlation criterion for establishing the physical validity of solutions is given.

## CONTENTS

	<u>Page</u>
Abstract . . . . .	iii
INTRODUCTION . . . . .	1
GIVEN DATA . . . . .	3
PROCEDURE . . . . .	4
DISCUSSION AND PRELIMINARY RESULTS . . . . .	13
ACKNOWLEDGMENT . . . . .	18
REFERENCES . . . . .	19

## INTRODUCTION:

The Goddard X-ray and extreme ultraviolet spectrograph on the seventh Orbiting Solar Observatory scanned the sun and its corona during the period October 2, 1971 to July 6, 1974, producing spectroheliograms in selected wavelengths corresponding to known, optically thin, emission lines emitted by coronal ions [1]. In addition to "large raster" spectroheliograms covering the whole sun, "small raster" spectroheliograms about five arc-minutes on a side were obtained which provided intensity distributions for particular active regions. A typical small raster contour plot is shown in Figure 1. In the case of many active regions, a large number of such rasters were obtained at a given wavelength over a period of days as the region rotated across the solar disk. The availability of these successive images or projections prompted the present study to determine whether the three-dimensional emission distribution within an active region can be reconstructed from a pair of OSO-7 rasters. This article is an interim report on the calculation, which during the past year has been carried to the point where it may be possible to determine the feasibility, or otherwise, of such a reconstruction from the available data. The calculation was developed independently of similar methods in other fields (e.g. the medical field, in which striking advances have recently been reported (reference [2], and other references in the same issue of IEEE Trans. on Nuclear Science)), but relationships will be discussed below. Two difficulties are encountered here beyond those dealt with by image reconstruction techniques in the laboratory. First, the source distribution is not necessarily constant with time, as well as possessing no distinct boundaries either within or without.

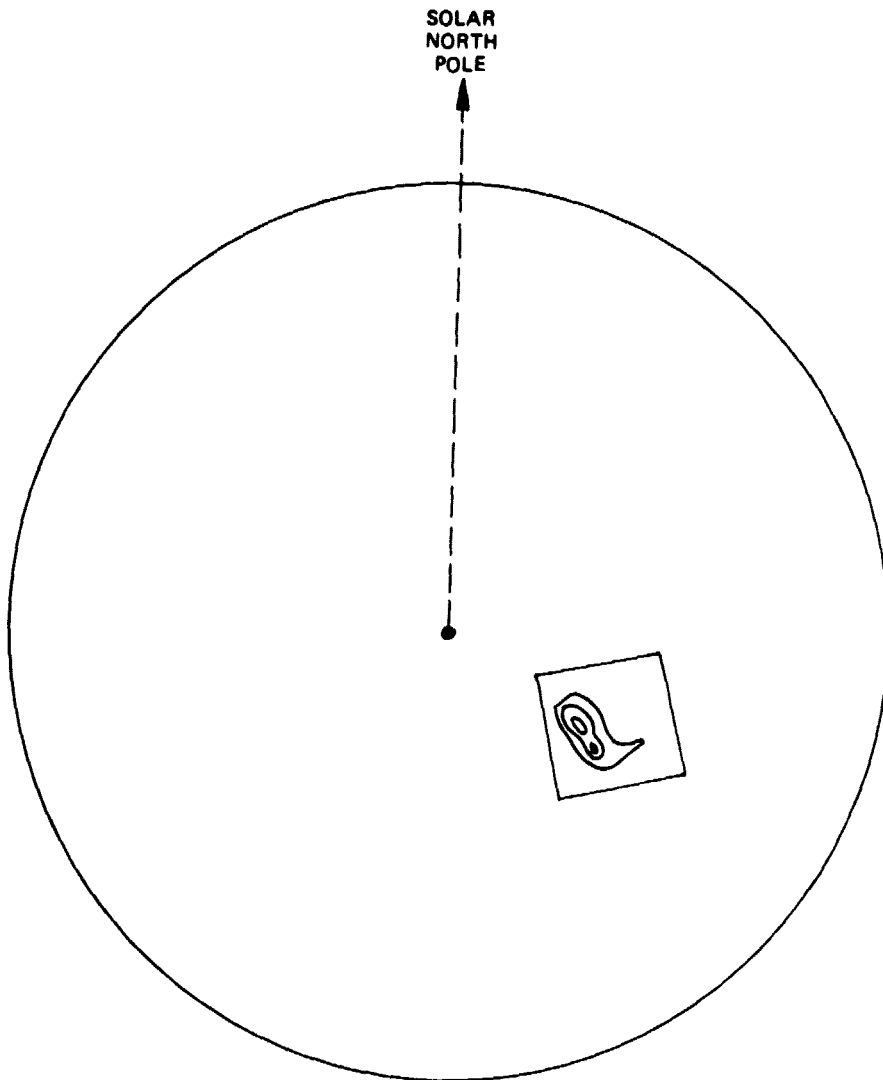


**Figure 1.** The small square projected here on the solar disc represents a typical OSO-7 small raster spectroheliogram observed in the Fe XV emission line wavelength  $284.1\text{\AA}$ . This particular raster, obtained on January 22, 1972, shows intensity contours of the active region McMath No. 11693.

Second, the solar rotation rate is not well known at coronal levels. Thus the general difficulty of the problem has been greater than anticipated. In the course of the calculation, however, a three-dimensional lattice of points is constructed which can be superimposed on an active region at different times and has proved to be useful for the investigation of its rotation.

Much of the calculation consists of basic geometrical and transformational steps which will be included for completeness.

#### GIVEN DATA:

The original OSO-7 measurements consist of a 23 x 16 irregular array of intensity elements over a total field of view of approximately 5 x 5 arc minutes for each small raster, which requires about one minute of time to record. For non-flaring active regions, up to twenty individual rasters are melded together to improve statistical accuracy. Then the elements are interpolated to produce a uniform array of 2500 intensity values  $I(i,j)$ ,  $i$  and  $j$  each taking values from 1 to 50, with an equal angular spacing of 6 arc seconds between points. Two such melded rasters, recorded at successive times such that a suitable solar angle separates them, are used in the following analysis and will be referred to as rasters A and B. Associated pertinent information is included with each of these melded rasters on a computer tape, such as: heliocentric coordinates of the central point  $(r_c, \theta_c)$  and four corner points  $(r_1, \theta_1; r_2, \theta_2; r_3, \theta_3; r_4, \theta_4)$ ; times of beginning and end of the period covered by the individual rasters included in the meld; solar pole position angle  $P$  and sub-earth solar longitude  $B_0$ .



## PROCEDURE:

A basic coordinate system, used throughout the calculation, was constructed as shown in Figure 2, with the sun's center as origin, x-axis passing through the earth, and z-axis directed toward an arbitrary direction here taken to be the projection of celestial north. (The computations are somewhat simplified if the projection of the solar north direction is taken as the z-axis, since P is then zero throughout, but the calculation is presented here as it was carried out.) The rasters A and B are considered to be two-dimensional images lying in the (y,z) plane. First raster A will be dealt with.

### 1. Use of raster A:

The coordinates of the center point and corner points of raster A are given by:

$$\begin{aligned}(y_c, z_c) &= (-r_c \sin(\theta_c + P), r_c \cos(\theta_c + P)) \\(y_1, z_1) &= (-r_1 \sin(\theta_1 + P), r_1 \cos(\theta_1 + P)) \\(y_2, z_2) &= (-r_2 \sin(\theta_2 + P), r_2 \cos(\theta_2 + P)) \\(y_3, z_3) &= (-r_3 \sin(\theta_3 + P), r_3 \cos(\theta_3 + P)) \\(y_4, z_4) &= (-r_4 \sin(\theta_4 + P), r_4 \cos(\theta_4 + P))\end{aligned}\tag{1}$$

Using these coordinates a two-dimensional grid of  $N_1 \times N_2$  points  $(y_{p,q}; z_{p,q})$  lying within the raster is constructed in the following way. The lengths of the sides of the raster are given by  $l_1 = [(y_2 - y_3)^2 + (z_2 - z_3)^2]^{\frac{1}{2}}$ ,  $l_2 = [(y_4 - y_3)^2 + (z_4 - z_3)^2]^{\frac{1}{2}}$  while the slopes of the sides are  $m_1 = (z_3 - z_2)/(y_3 - y_2)$  and  $m_2 = (z_3 - z_4)/(y_3 - y_4)$ . Choosing the distances between the grid points as  $\Delta l_1 = K_1 l_1/(N_1 + 1)$ ,  $\Delta l_2 = K_2 l_2/(N_2 + 1)$ , with  $K_1$  and  $K_2$  as desired fractions of the raster dimensions to be covered

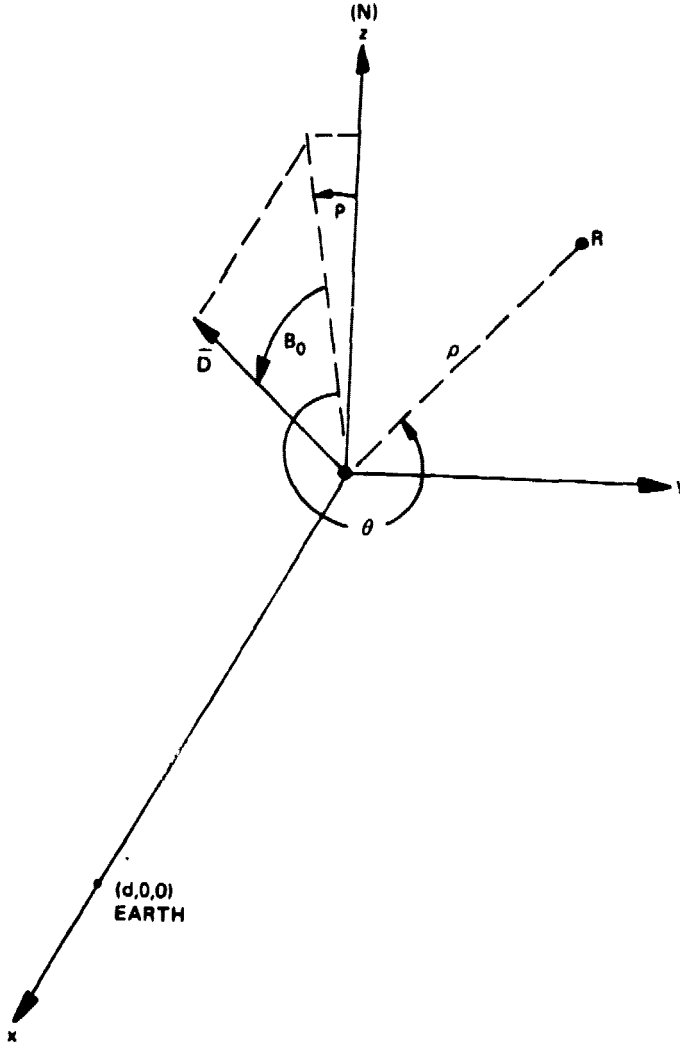


Figure 2. Coordinate system used in the text, with origin at the center of the Sun, z axis in the direction of celestial north, earth observer at the point  $(d, 0, 0)$  on the x axis.  $\bar{D}$  represents the solar rotation axis, of which the projection on the  $(y, z)$  plane lies at the angle  $P$  to the north direction;  $\bar{D}$  is tilted out of the  $(y, z)$  plane by the angle  $B_0$ . A detailed discussion of the solar parameters  $P$  and  $B_0$  may be found on pages 307-9 of reference (8).  $R$  represents an observed point in an EUV raster, lying in the  $(y, z)$  plane and defined by the solar disc coordinates  $(\rho, \theta)$ .

by the grid, a first grid point is constructed as:

$$y_{1,1} = \text{sign}(y_3 - y_4) [\frac{1}{2}(N_2 - 1) \Delta l_2 / (1 + m_2^{-2})^{\frac{1}{2}}] \\ + \text{sign}(y_3 - y_2) [\frac{1}{2}(N_1 - 1) \Delta l_1 / (1 + m_1^{-2})^{\frac{1}{2}}] \quad (2a)$$

$$z_{1,1} = (\text{similarly})$$

Points  $(y_{p,1}; z_{p,1})$  are then constructed as

$$y_{p,1} = \text{sign}(y_2 - y_3) [(p - 1) \Delta l_1 / (1 + m_1^{-2})^{\frac{1}{2}}] + y_{1,1} \quad (2b)$$

$$z_{p,1} = (\text{similarly})$$

and general points  $(y_{p,q}; z_{p,q})$  are further constructed according to

$$y_{p,q} = \text{sign}(y_4 - y_3) [(q - 1) \Delta l_2 / (1 + m_2^{-2})^{\frac{1}{2}}] + y_{p,1} \quad (2c)$$

$$z_{p,q} = (\text{similarly})$$

This produces the desired two-dimensional grid, centered within raster A.

Corresponding polar coordinates of these points in the  $(y,z)$  plane are

$$\rho_{p,q} = [y_{p,q}^2 + z_{p,q}^2]^{\frac{1}{2}} \quad (3) \\ \theta_{p,q} = \tan^{-1}[-y_{p,q}/z_{p,q}]$$

These grid polar coordinates are next used to produce a three-dimensional lattice of  $N_1 \times N_2 \times N_3$  points  $(x_{pqr}, y_{pqr}, z_{pqr})$  extending throughout the volume of solar atmosphere viewed by the raster, consisting of successive two-dimensional grids separated by a chosen distance  $l$ :

$$x_{p,q,r} = \frac{d\rho_{p,q}^2 + d[\rho_{p,q}^4 + (d^2 + \rho_{p,q}^2)((1 + r\ell)^2 - \rho_{p,q}^2)]^{\frac{1}{2}}}{d^2 + \rho_{p,q}^2} \\ y_{p,q,r} = -[\rho_{p,q}(d - x_{p,q,r}) \sin \theta_{p,q}]/d \quad (4) \\ z_{p,q,r} = [\rho_{p,q}(d - x_{p,q,r}) \cos \theta_{p,q}]/d$$

$d$  being the earth-sun distance in solar radii.

In this lattice, successive points  $(p,q,r)$ ,  $(p,q,r+1)$ ,  $(p,q,r+2)$ , ... lie along a line of sight joining the earth (observer) to the point  $(y_{p,q}; z_{p,q})$  lying in the  $(y,z)$  plane (see Figure 3); thus the lattice, composed of  $N_1 \times N_2$  such lines converging to the earth, is not exactly a cubic lattice but departs from parallelism by the small angle of less than 1 arc-minute or 0.0003 radian existing between the lines. For the present purpose this small departure can be neglected.

The solar latitude  $B_{pqr}$  and the height  $H_{pqr}$  above the surface of each of the lattice points is given by

$$B_{p,q,r} = (1 + r\ell)^{-1} \sin^{-1} [x_{p,q,r} \sin B_0 - y_{p,q,r} \sin P \cos B_0 + z_{p,q,r} \cos P \cos B_0] \quad (5)$$

$$H_{p,q,r} = (6.9598 \times 10^5) r\ell \quad (\text{in km})$$

The volume of solar atmosphere encompassed by this lattice may be considered to be composed of discrete rectangular source blocks, each centered on a lattice point  $(x_{pqr}, y_{pqr}, z_{pqr})$ , so that along a line of sight  $(p,q)$  the total intensity  $I_{p,q}$  emitted toward the observer is the sum of separate contributions  $S(p,q,r)$ ,  $S(p,q,r+1)$ ,  $S(p,q,r+2)$  ... emitted by the source blocks centered on the corresponding lattice points; thus  $I_{p,q}$  emerges from the end of a source column of rectangular cross-section whose axis is the line of sight  $(p,q)$ . To obtain  $I_{p,q}$  from the actual raster intensities  $I(i,j)$ , the latter values are summed over values of  $i,j$  which lie within the cross-section of the source column. In this step the following equivalence between raster indices  $(i,j)$  and rectangular

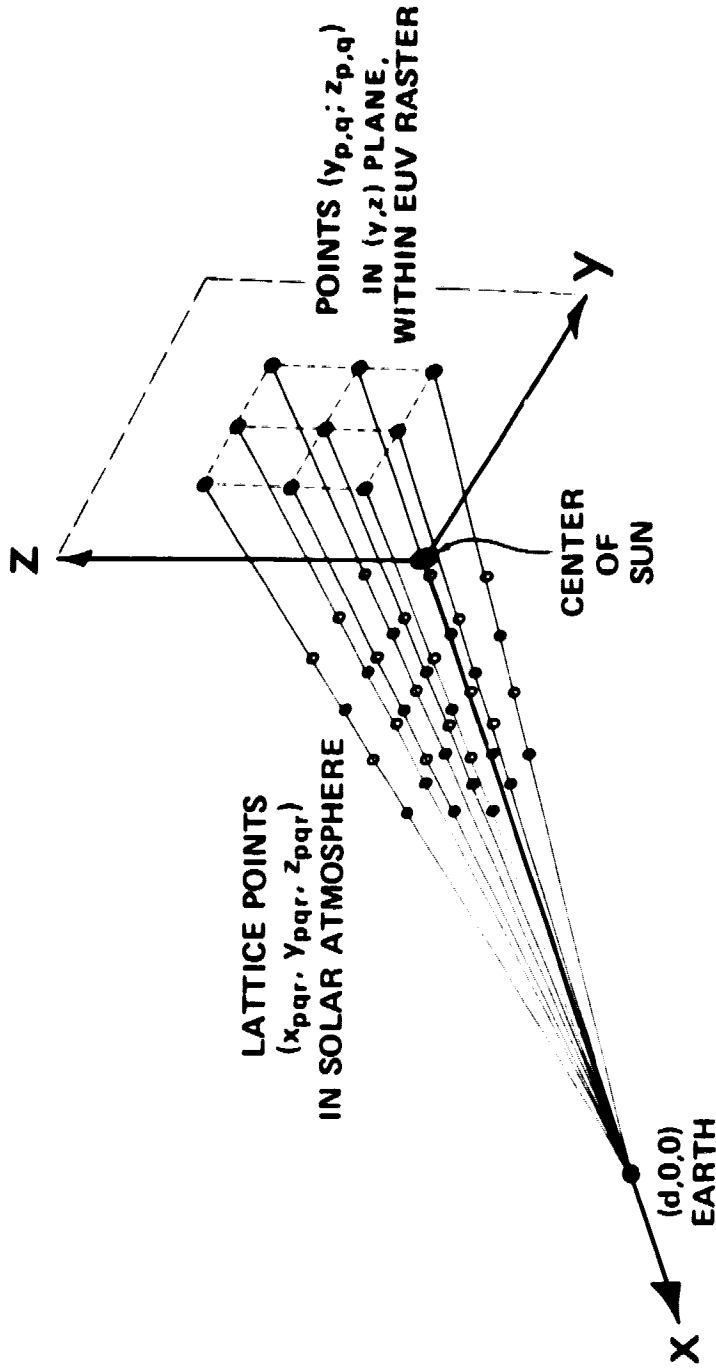


Figure 3. This figure illustrates, in a schematic way, the relation of the lattice points given by equations (4) to the original grid points (2).

coordinates (y,z) is needed:

$$y(i,j) = \frac{2i-1}{100} [y_3 + \frac{1}{100} (2j-1)(y_4 - y_3)] + (1 - \frac{2i-1}{100}) [y_2 + \frac{1}{100} (2j-1)(y_1 - y_2)]$$

$$z(i,j) = (\text{similarly}) \tag{6}$$

Now, by transforming from the triplet of variables p,q,r to two new variables t,i by the transformation

$$t = N_2(p - 1) + q$$

$$i = N_2 N_1(p - 1) + N_3(q-1) + r \tag{7}$$

a set of linear equations is constructed which expresses the fact that each intensity value  $I_{p,q} \equiv I_t$  corresponds to a source column t composed of contributions  $S_{t,i}, S_{t,i+1}, S_{t,i+2}, \dots$ :

$$I(1) = S(1,1) + S(1,2) + \dots + S(1,N_3)$$

$$I(2) = S(2,N_3 + 1) + S(2,N_3+2) \dots + S(2,2N_3)$$

$$\vdots$$

$$I(N_1 N_2) = S(N_1 N_2, N_1 N_2 N_3 - N_3 + 1) + \dots + S(N_1 N_2, N_1 N_2 N_3) \tag{8}$$

## 2. Use of raster B:

Since the active region registered on raster A at time  $t_A$  has rotated through an angle  $\delta \approx 360((t_B - t_A)/24)$  about the solar axis by the time it is registered on raster B at time  $t_B$ , one must rotate the lattice blocks centered on  $(x_{pqr}, y_{pqr}, z_{pqr})$  by the same amount and around the same axis. The rotation of a vector  $\vec{r}$  through an angle  $\delta$  about an arbitrary axis  $\vec{D}$ , in a clockwise direction when viewed along the positive direction

of  $\bar{D}$ , is given by the transformation [3]:

$$\bar{r}' = \bar{r} + \sin \delta (\bar{D} \times \bar{r}) + (1 - \cos \delta) (\bar{D} \times (\bar{D} \times \bar{r})) \quad (9)$$

Application of this rotation to the original lattice points  $(x_{pqr}, y_{pqr}, z_{pqr})$  results in the new lattice  $(X_{pqr}, Y_{pqr}, Z_{pqr})$  superimposed on the active region in its later position, as registered in raster B:

$$\begin{aligned} X_{p,q,r} &= x_{pqr} + (\beta_D \cdot z_{pqr} - \gamma_D \cdot y_{pqr}) \sin \delta_{pqr} \\ &\quad + (1 - \cos \delta_{pqr}) [\beta_D (\alpha_D \cdot y_{pqr} - \beta_D \cdot x_{pqr}) - \gamma_D (\gamma_D \cdot x_{pqr} - \alpha_D \cdot z_{pqr})] \\ Y_{p,q,r} &= y_{pqr} + (\gamma_D \cdot x_{pqr} - \alpha_D \cdot z_{pqr}) \sin \delta_{pqr} \\ &\quad + (1 - \cos \delta_{pqr}) [\gamma_D (\beta_D \cdot z_{pqr} - \gamma_D \cdot y_{pqr}) - \alpha_D (\alpha_D \cdot y_{pqr} - \beta_D \cdot x_{pqr})] \\ Z_{p,q,r} &= z_{pqr} + (\alpha_D \cdot y_{pqr} - \beta_D \cdot x_{pqr}) \sin \delta_{pqr} \\ &\quad + (1 - \cos \delta_{pqr}) [\alpha_D (\gamma_D \cdot x_{pqr} - \alpha_D \cdot z_{pqr}) - \beta_D (\beta_D \cdot z_{pqr} - \gamma_D \cdot y_{pqr})] \end{aligned} \quad (10)$$

where  $\alpha_D = \sin B_0$ ,  $\beta_D = -\sin P \cos B_0$ ,  $\gamma_D = \cos P \cos B_0$ , and the rotation angle  $\delta_{pqr}$  - a function of the latitude  $B_{pqr}$  of each point - has been taken here initially to be a function of the form  $a + b \sin^2 B_{pqr}$ , based on the latitude dependence of solar rotation which is generally accepted in the literature. Remarks on the importance, for this calculation, of finding a correct function to represent  $\delta_{pqr}$  will be made in concluding sections.

The corners of each source block centered on a given lattice point  $(x_{pqr}, y_{pqr}, z_{pqr})$  are similarly rotated into their new positions. With

the aid of the new corner coordinates, the equations of the six bounding planes of a given source block may be obtained; for convenience we denote them here as:

$$\begin{aligned}
 a_1x + b_1y + c_1z + d_1 &= 0; & a_4x + b_4y + c_4z + d_4 &= 0 \\
 a_2x + b_2y + c_2z + d_2 &= 0; & a_5x + b_5y + c_5z + d_5 &= 0 \\
 a_3x + b_3y + c_3z + d_3 &= 0; & a_6x + b_6y + c_6z + d_6 &= 0
 \end{aligned} \tag{11}$$

Now, unlike the simpler situation existing in the case of raster A, a line of sight to the point  $(X_{pqr}, Y_{pqr}, Z_{pqr})$  does not intersect any other point  $(X_{p'q'r'}, Y_{p'q'r'}, Z_{p'q'r'})$  in general, so that a corresponding observing cylinder of rectangular cross-section will intercept the source blocks along its path in various fractional volumes. Thus such an observing cylinder  $(p,q,r)$ , corresponding to an observed intensity  $I_{p,q,r}$ , will intersect a certain volume  $V_{p,q,r}$  of the source block centered on  $(X_{pqr}, Y_{pqr}, Z_{pqr})$ , and will intersect other source blocks  $(X_{uvw}, Y_{uvw}, Z_{uvw})$  in the vicinity of the line of sight in further particular volumes  $V_{uvw}$ . If the full volume of a source block is  $V_0$ , then the contribution of source block  $(X_{pqr}, Y_{pqr}, Z_{pqr})$  to the observed intensity  $I_{p,q,r}$  is  $V_{pqr}/V_0$ , and similarly the contributions of neighboring blocks  $(u,v,w)$  are  $V_{uvw}/V_0$ . These contributions will then all be less than unity.

The four planes bounding a typical observing cylinder may be written for conciseness as:

$$\begin{aligned}
 a_7x + b_7y + c_7z + d_7 &= 0; & a_9x + b_9y + c_9z + d_9 &= 0 \\
 a_8x + b_8y + c_8z + d_8 &= 0; & a_{10}x + b_{10}y + c_{10}z + d_{10} &= 0
 \end{aligned} \tag{12}$$



To obtain the actual value of the volume of intersection of observing cylinder and source block - specified by the intersection of the set of planes (11) with the set of planes (12) - a Monte Carlo procedure is used in which random points are thrown into the source block, and the numbers of these points which also fall within the observing cylinder are counted. (This turns out to be a difficult problem to solve analytically.)

The contributions  $V_{pqr}/V_0$  and  $V_{uvw}/V_0$  are just the coefficients  $a_{t,i}$  required in a set of linear equations which state that the observed intensities  $I_{p,q,r}$  (obtained by appropriately summing intensities  $I(i,j)$  of raster B over the cross-section of observing column  $(p,q,r)$ , as was done for raster A) are sums of source contributions along the line of sight to the point  $(p,q,r)$ , and which will be added to the first set constructed for raster A. To formulate this additional set we transform from the variables  $(p,q,r)$  to the variable  $t$  by the relation:

$$t = N_1 N_2 + N_2 N_3(p-1) + N_3(q-1) + r \quad (13)$$

with the relation between  $i$  and  $(p,q,r)$  remaining as in (7). This results in the set:

$$\begin{aligned} I(N_1 N_2 + 1) &= \sum_i a(N_1 N_2 + 1, i) S(N_1 N_2 + 1, i) \\ I(N_1 N_2 + 2) &= \sum_i a(N_1 N_2 + 2, i) S(N_1 N_2 + 2, i) \\ &\vdots \\ I(N_1 N_2 + N_1 N_2 N_3) &= \sum_i a(N_1 N_2 + N_1 N_2 N_3, i) S(N_1 N_2 + N_1 N_2 N_3, i) \end{aligned} \quad (14)$$

with  $i$  taking values from 1 to  $N_1 N_2 N_3$  as before.

These equations, together with the first set (8), can be represented by the following full matrix equation for the unknown source vector  $\bar{S}$  whose elements are the emission strengths of the individual source blocks:

$$\bar{I} = |A|\bar{S} \quad , \quad (15)$$

in which the coefficient matrix  $|A|$ , a sparse matrix, is of dimensions  $(N_1 N_2 + N_1 N_2 N_3) \times (N_1 N_2 N_3)$ . The general form of  $|A|$  can be represented schematically as in Figure 3.

#### DISCUSSION AND PRELIMINARY RESULTS:

##### 1. Relationship to other three-dimensional reconstruction methods:

Gordon and Herman [4] classify existing three-dimensional reconstruction methods into four main categories: summation, use of Fourier transforms, analytic solution of integral equations, and series expansion approaches. Budinger and Gullberg [2] expand this classification further into thirteen detailed procedures, one of which consists of direct matrix and linear equation methods (included within the series expansion approaches described by Gordon and Herman). The present calculation falls into this category which is discussed in a physically meaningful way by Budinger and Gullberg. Further, it deals with a "situation where we are limited in the number of views" in which Budinger and Gullberg note that the resulting matrix may be close to singular, and may therefore require for its solution the use of iterative methods.

Direct inversions of the coefficient matrix  $|A|$  have been attempted, as a first trial, for pairs of rasters separated by solar rotation angles from  $15^\circ$  to  $47^\circ$ . The three-dimensional lattice used was  $5 \times 5 \times 5$ , giving

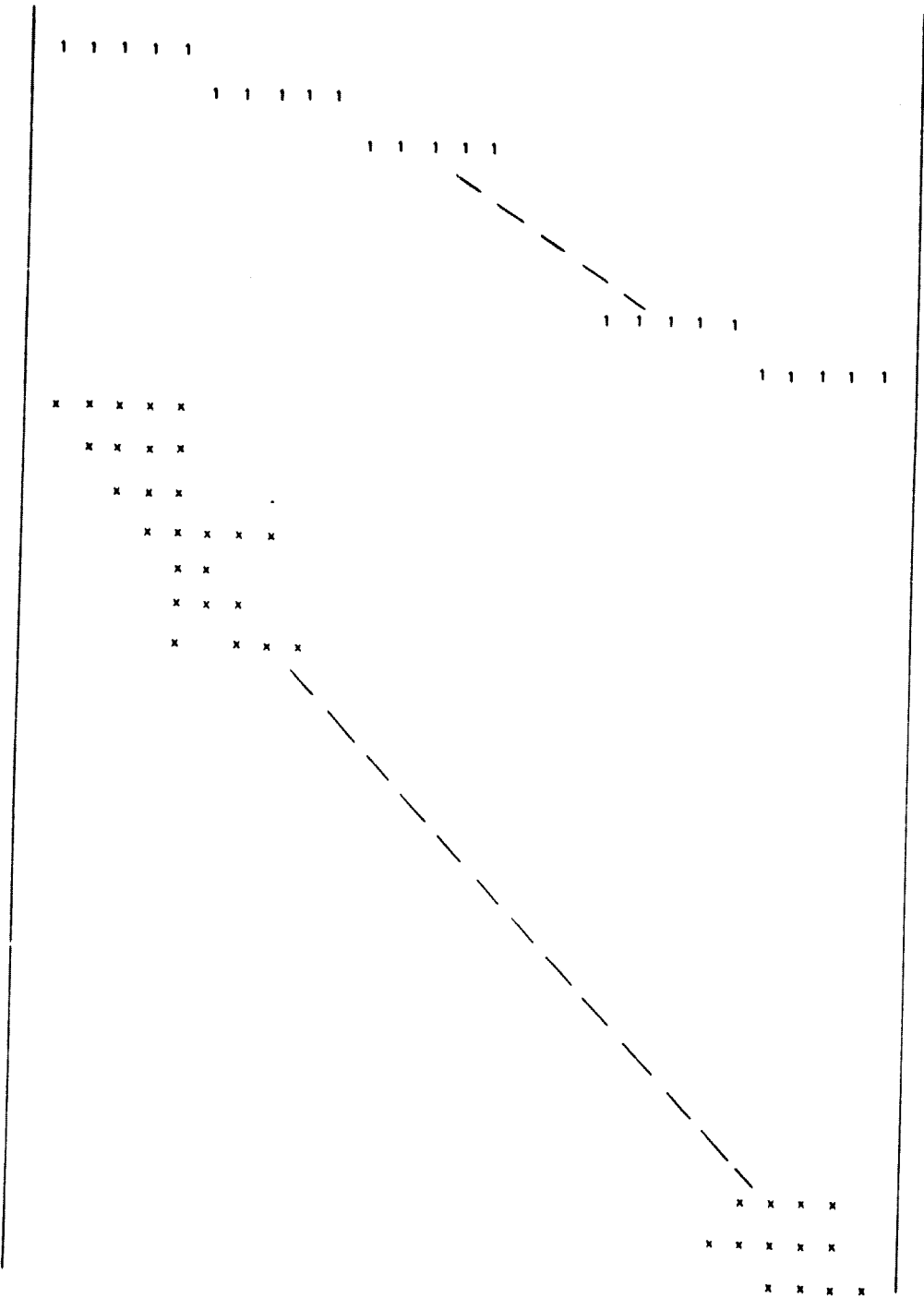


**Figure 4.** General appearance of the final coefficient matrix  $A$ ; the non-zero elements denoted by  $x$  have values between zero and unity. All elements other than unity or  $x$  are zero.

dimensions of  $125 \times 150$  for  $|A|$ . Unique solution vectors  $S$ , in the mathematical sense of satisfying the original equation (15), are obtained which however possess some negative - nonphysical - elements. These solutions may nevertheless contain some physical reality. (In this connection one may note that a standard procedure in some of the ART (algebraic reconstruction techniques) algorithms [2], [4] is to set negative elements equal to zero.) We are now at a stage in the calculation in which it may be possible to assess the reality, or non-reality, of these solutions. A correlation method which we expect to use for this purpose, and whose general principle does not appear to have been suggested previously, is described in the following section.

## 2. A Correlation Criterion for Validity of the Solution:

When a solution  $S(x_{pqr}, y_{pqr}, z_{pqr})$  of the matrix equation (15) is obtained, one would like to establish whether it is a physically valid solution or not. This is not a trivial problem in the case at hand, since active region distributions are expected to be diffuse rather than compact, as mentioned in the Introduction where it was noted that in this respect the present problem is more difficult than the medical three-dimensional reconstruction problem. A correlation method is described here which may be of general interest in such cases. The method consists of running the calculation, on a given pair of rasters, with successively decreasing grid sizes which produce corresponding solution sets  $S^a(x^a_{pqr}, y^a_{pqr}, z^a_{pqr})$ ,  $S^b(x^b_{pqr}, y^b_{pqr}, z^b_{pqr})$ ,  $S^c(x^c_{pqr}, y^c_{pqr}, z^c_{pqr})$ ,.... For a given pair of solution sets, say  $S^a$  and  $S^b$ , one first interpolates the function  $S^a(x^a_{pqr}, y^a_{pqr}, z^a_{pqr})$  to find its values  $S^a(x^b_{pqr}, y^b_{pqr}, z^b_{pqr})$  at

the lattice points of the second solution  $S^b$ . For a given  $r$  - i.e. for a given height in the solar atmosphere - the following normalized correlation coefficient is then constructed:

$$\Gamma_r(a,b) = \frac{\sum_{p,q} S^b(x^b_{pqr}, y^b_{pqr}, z^b_{pqr}) \cdot S^a(x^a_{pqr}, y^a_{pqr}, z^a_{pqr})}{\sum_{p,q} [S^>(x^b_{pqr}, y^b_{pqr}, z^b_{pqr})]^2} \quad (16)$$

where  $S^>$  represents the larger of  $S^a$  or  $S^b$ . This coefficient is seen to approach unity the more closely the solution field  $S^a$  resembles the solution field  $S^b$ . The final overall parameter describing the correlation of solution  $S^a$  with  $S^b$  is then  $\Gamma(a,b) = \sum_r \Gamma_r(a,b)$ . The hypothesis underlying the use of this parameter is that a physically valid solution field will be independent of the size of the lattice used. It is expected to be of value for example in improving the trial rotation period used in the calculation, since one can vary the assumed rotation period so as to maximize  $\Gamma(a,b)$  or more generally the quantity  $\Gamma_{total} = \sum_{j>i} \Gamma(i,j)$ .

### 3. Requirements imposed by the data:

The present procedure could be extended to include more than two projections (rasters) without undue difficulty, but two projections only were used in this first attempt because of limitations imposed by the nature of the solar sources dealt with. An ideal source region, for the purpose of this inversion calculation, would possess the following properties:

- (a) the source distribution should remain reasonably constant with time;
- (b) its emission should be much greater than that of any background which is present;
- (c) its size should be appreciably less than the raster size, i.e. than the cross-section of the observing "beam"; and

(d) its rotation rate should be accurately known. Actual solar active regions fall short of the ideal in all of these respects. The solar rotation rate is known only to a first approximation, being a function of several variables such as solar latitude, altitude above the solar surface, type of feature considered (sunspots, coronal features, magnetic features, etc.). Recent papers which give further references on this topic are those of Henze and Dupree [5] and Simon and Noyes [6]. The present uncertainty which exists in the field may be illustrated by the fact that while Simon and Noyes find "constancy of rotational rate between chromosphere and corona" and Henze and Dupree similarly "cannot discern a variation in rotation rate between chromosphere and corona", El-Raey and Scherrer [7] find that "the upper chromosphere and lower corona rotate from 5 to 8% faster than either the photosphere or corona". On the other hand, since the present calculation requires an accurate solar rotation function as input for a successful solution, it also has the potential of establishing such a function unambiguously.

The further limitations imposed by conditions (a), (b) and (c) above are presently being explored in the OSO-7 data.

**ACKNOWLEDGMENT:**

The authors wish to thank Werner M. Neupert and Charles E. Condor for their support and assistance with the interpretation of the OSO-7 data.

## REFERENCES

1. J. H. Underwood and W. M. Neupert, Solar Phys. 35(1974), 241.
2. T. F. Budinger and G. T. Gullberg, IEEE Trans. on Nuclear Science, Vol. NS-21, No. 3(1974),2.
3. P. I. Richards, Manual of Mathematical Physics, Pergamon Press, London, 1959, p. 292.
4. R. Gordon and G. T. Herman, International Review of Cytology 38 (1974), 111.
5. W. Henze and A. K. Dupree, Solar Phys. 33 (1973), 425.
6. G. W. Simon and R. W. Noyes, Solar Phys. 26 (1972), 8.
7. M. El-Raey and P. H. Scherrer, Solar Phys. 26 (1972), 15.
8. Explanatory Supplement to the Astronomical Ephemeris and The American Ephemeris and Nautical Almanac (London, Her Majesty's Stationery Office) 1974.